

Physical Constraints on Motility with Applications to Possible Life on Mars and Enceladus

MANASVI LINGAM^{1,2} AND ABRAHAM LOEB²

¹*Department of Aerospace, Physics and Space Sciences, Florida Institute of Technology, Melbourne FL 32901, USA*

²*Institute for Theory and Computation, Harvard University, Cambridge MA 02138, USA*

ABSTRACT

Motility is a ubiquitous feature of microbial life on Earth, and is widely regarded as a promising biosignature candidate. In the search for motile organisms, it is therefore valuable to have rough estimates for the number of such microbes that one may expect to find in a given area or volume. In this work, we explore this question by employing a simple theoretical model that takes into account the amount of free energy available in a given environment and the energetic cost of motility. We present heuristic upper bounds for the average biomass density and the number density of motile lifeforms for the Martian subsurface and the ocean of Enceladus by presuming that the motile microbes in question derive their energy from methanogenesis. We consequently demonstrate that the resultant densities of motile organisms might be potentially comparable to, or much lower than, the total microbial densities documented in various extreme environments on Earth.

1. INTRODUCTION

Motility is a common characteristic of microorganisms on Earth. It is suspected that $\sim 20\%$ of all bacteria on Earth are motile (Fenchel 2008), but the exact fraction is uncertain by more than one order of magnitude (Azam & Malfatti 2007). It has been hypothesized that motility is likely to constitute a generic feature of microbes in aquatic environments (Nadeau et al. 2016, pg. 758). There are sound reasons as to why the study of motility in generic astrobiological settings is desirable. For starters, the effective diffusion coefficient associated with motility is orders of magnitude higher than non-motile organisms if the putative organisms have radii of $\gtrsim 1 \mu\text{m}$ (Dusenbery 2009, pg. 176). On a related note, it is well known that motility, in tandem with chemotaxis, facilitates a substantive increase in nutrient uptake (Stocker 2012, pg. 629).

At the same time, however, motility does incur significant energetic costs, which take up a considerable fraction of the total organismal metabolic budget (Taylor & Stocker 2012, pg. 678). Therefore, in theoretical studies that seek to assess habitability and the putative density of microbes from the standpoint of energetics (Hoehler 2007; Shock & Holland 2007; Higgins & Cockell 2020), it is arguably necessary to incorporate these costs in a self-consistent fashion (Van Bodegom 2007). Last, from the perspective of *in situ* life-detection missions, motility comprises a viable biosignature candidate (Neveu et al.

2020; Lingam & Loeb 2021; Riekes et al. 2021). In fact, the spatial resolution that would be required to identify motile organisms is effectively lower compared with their nonmotile counterparts (Nadeau et al. 2016, pg. 755).

It is thus valuable to place constraints on the maximum global biomass density and number density of motile microbes in a given habitat, as this can guide us in the design of life-detection experiments. Moreover, obtaining such estimates is helpful from the standpoint of empirically assessing the model because these constitute clear predictions that could be testable by future missions in principle. Hence, in this work, we select two representative habitable environments—the Martian subsurface (Michalski et al. 2018) and the ocean of Enceladus (Hand et al. 2020), both of which are regarded as being habitable and have been subjected to extensive analysis—and calculate heuristic upper bounds on the densities of motile organisms in these particular settings.

The outline of the paper is as follows. In Sec. 2, we provide a brief description of the model used to compute the power requirements for motility. Next, we apply a simple energetic model to estimate the maximal biomass and number density in Sec. 3. Finally, we summarize the salient findings and caveats in Sec. 4.

2. MODEL DESCRIPTION FOR MOTILE ORGANISMS

Microbes on Earth have evolved a multitude of strategies for motility, each of which is attuned to the specifics of the habitats that they inhabit (Berg 1993). Hence, we preface our analysis with the caveat that our results

may have limited applicability in certain settings. Our results are, however, reasonably valid in microenvironments that are characterized by low Reynolds numbers; under such conditions, the prevalent mode of motility is taken to be run-and-tumble chemotaxis (Kempes et al. 2019, Section 4.2). To calculate the accompanying energetic cost, we will mirror the formalism presented in Mitchell (2002); see also Berg (1993) for additional quantitative details. In Appendix A, we provide a detailed synopsis of the challenges associated with formulating quantitative models of motility and our rationale for working with run-and-tumble chemotaxis hereafter.

In the case of run-and-tumble chemotaxis, the total energetic cost of motility (units of W/cell), denoted by P_m , can be decomposed into two components as follows:

$$P_m = P_{rp} + P_{tp}, \quad (1)$$

where the subscripts “ r ” and “ t ” signify the running (swimming) and tumbling (reorientation) phases, respectively. The expression for the swimming phase (P_{rp}) is given by the first term on the right-hand side of Mitchell (2002, their Equation 6), which is expressible as

$$P_{rp} \approx \frac{k_B T D_s}{R^2}, \quad (2)$$

where T is the temperature, D_s denotes the molecular diffusivity of the solvent, and R represents the radius of the cell. Over the habitable range of temperatures associated with life-as-we-know-it, both T and D_s vary by a factor relatively close to unity. Hence, we adopt the fiducial values of $D_s \approx 10^{-9} \text{ m}^2 \text{ s}^{-1}$ and $T \approx 300 \text{ K}$ (Holz et al. 2000). By substituting these estimates into the equation for P_{rp} , we arrive at

$$P_{rp} \approx 4.1 \times 10^{-18} \text{ W} \left(\frac{R}{1 \mu\text{m}} \right)^{-2}. \quad (3)$$

By proceeding in a similar vein to calculate P_{tp} , we make use of the relations in Mitchell (2002, pg. 730) and Mitchell (1991, pg. 229), which collectively yield

$$P_{tp} \approx 3 \times 10^{-19} \text{ W} \left(\frac{R}{1 \mu\text{m}} \right)^3. \quad (4)$$

Hence, by substituting (4) and (3) in (1), we ascertain that P_m becomes significant when $R \gg 1 \mu\text{m}$ as well as when R approaches the lower limit associated with microbes on Earth. The latter trend is consistent with the observation that $\gtrsim 10\%$ of the energy per unit time derived from metabolism is expended on motility by smaller bacteria (Mitchell 1991).

By calculating $dP_m/dR = 0$, the minimum is attained at $R_c \approx 1.6 \mu\text{m}$ and the corresponding value of P_m at $R = R_c$ is $P_c \approx 2.8 \times 10^{-18} \text{ W}$. As a point of comparison, the minimum power per cell required for maintenance, as predicted by both state-of-the-art models and empirical data, is $P_{\min} \approx 10^{-21} \text{ W}$ (Bradley et al. 2020). There are

two important points to bear in mind with regards to R_c and P_c . First, neither of them are strictly constants, as they actually exhibit a weak dependence on D_s and T . Second, for life-as-we-know-it, because neither of these two environmental parameters are subject to significant variation, it is conceivable that both R_c and P_c may evince a certain degree of generality.

3. MAXIMUM BIOMASS FOR MOTILE ORGANISMS

We can estimate the *maximum* feasible biomass for chemoautotrophs (M_{\max}) by taking only the constraints from motility into account. The reason that we end up with an upper bound is because all the chemical energy is assumed to be utilized exclusively for the sake of motility in this simple model, and not toward the function of basal maintenance; the latter has a lower bound of P_{\min} . With this assumption, M_{\max} is given by

$$M_{\max} \approx \frac{C_{\text{cell}} |\Delta G| \Phi_{\max} A_{\text{bio}}}{P_{\text{bio}}}, \quad (5)$$

where P_{bio} represents the temporally averaged power required for a motile microbe, C_{cell} is the mass of the organism, ΔG is the net Gibbs free energy associated with the exergonic chemical reaction in the given environmental conditions, Φ_{\max} denotes the maximum flux of the appropriate reactant(s), and A_{bio} is the cross-sectional area of the putative biosphere (Seager et al. 2013; Sholes et al. 2019; Lingam & Loeb 2020).

The fraction of time spent by microbes in a state of motion is denoted by ϵ . The temporally averaged power expended by microbes on this activity is therefore roughly given by $P_{\text{bio}} \approx \epsilon P_m$. We adopt a characteristic value of $\epsilon \sim 0.1$, as many bacteria are known to evince $\epsilon \lesssim 0.2$ (Mitchell & Kogure 2006, pg. 12). In select environments, $\epsilon \ll 1$ could certainly be manifested—especially in energy-limited habitats that stymie the prospects for motility (Lever et al. 2015)—but we are interested in exploring the characteristics of moderately active and motile microbes; for these reasons, we shall hereafter employ $\epsilon \sim 0.1$. Next, we are free to adopt $C_{\text{cell}} \approx 4\pi\rho_w R^3/3$, where ρ_w is the density of water; this relation follows from the datum that the density of cells is close to that of water (Milo & Phillips 2016).

By plugging the above relations in (5), we arrive at

$$M_{\max} \propto \left[4.1 \left(\frac{R}{1 \mu\text{m}} \right)^{-5} + 0.3 \right]^{-1}, \quad (6)$$

where it is now necessary to interpret R as the characteristic radius of the ensemble of microbes present in a particular habitat. It is apparent that M_{\max} decreases monotonically with R , implying that most of the biomass is concentrated in the form of microbes with sizes of at least a few microns. This behavior stands in contradistinction to P_m , because the latter is a non-monotonic function of R , as demonstrated earlier. In

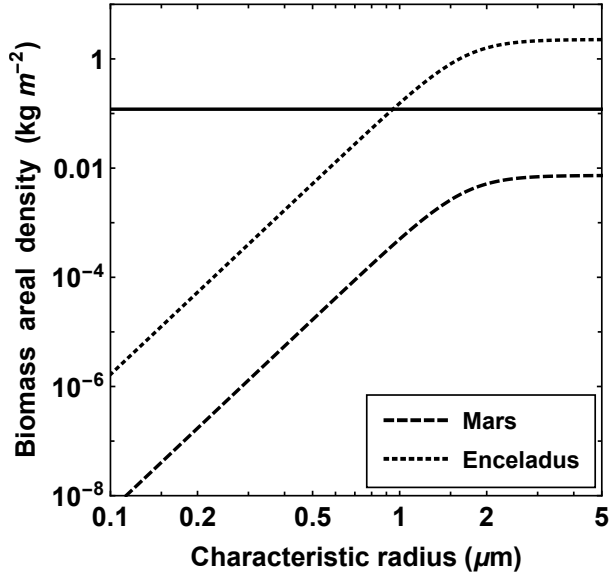


Figure 1. The upper bound on the total biomass of motile organisms per unit area (biomass areal density) in SI units of kg m^{-2} as a function of the microbe radius (in μm) for putative methanogens in the Martian subsurface and the ocean of Enceladus. These estimates were calculated for the fiducial choice of $\epsilon \sim 0.1$ in (7), which is the fraction of time spent in motion. The horizontal black line is an estimate of the biomass areal density of Earth’s deep biosphere.

contrast, let us suppose that we wish to calculate the number of microbes; this requires us to divide M_{max} with C_{cell} . After doing so, the result is inversely proportional to P_m . Hence, the upper bound on the number of motile cells attains a maximum when P_m is minimized: that is, when $R = R_c$ and $P_m = P_c$. In other words, the number of motile cells is maximized when the putative microbes exhibit a radius of $\sim 1.6 \mu\text{m}$, as explained in Sec. 2.

The other noteworthy aspect is that $M_{\text{max}} \propto A_{\text{bio}}$, as seen from (5), indicating that larger habitats/worlds are likely to host more biomass. Hence, it is more instructive to analyze the biomass areal density (i.e., vertically integrated biomass per unit area), defined as $\sigma_{\text{max}} = M_{\text{max}}/A_{\text{bio}}$. To calculate σ_{max} , it is imperative to consider a specific pathway and location. For the sake of comparison, we consider putative methanogen-like microbes. Our reasons are twofold. First, the reactants necessary for methanogens (viz., CO_2 and H_2) are widely available in many astrobiological environments, as the ensuing examples illustrate. Second, methanogens are capable of survival and growth in diverse conditions and have therefore served as model organisms in many experimental and theoretical analyses that were designed to emulate or simulate extraterrestrial settings (McKay & Smith 2005; Taubner et al. 2015, 2018; Higgins & Cockell 2020; Lingam & Loeb 2021).

The first setting that we consider is the Martian subsurface, because this was investigated in Sholes et al. (2019). Another point of significance is that liquid water mixtures have been confirmed in this environment (Wray 2021). On the basis of the simulations and data presented in Sholes et al. (2019), we normalize Φ_{max} by $\Phi_M \approx 1.3 \times 10^{12} \text{ m}^{-2} \text{ s}^{-1}$ and ΔG by $\Delta G_M \approx -24 \text{ kJ mol}^{-1}$, with the subscript “M” embodying the the Martian subsurface. After invoking (5), we end up with

$$\sigma_{\text{max}} \approx 2.2 \times 10^{-3} \text{ kg m}^{-2} \left(\frac{\Phi_{\text{max}}}{\Phi_M} \right) \left(\frac{|\Delta G|}{|\Delta G_M|} \right) \left(\frac{\epsilon}{0.1} \right)^{-1} \times \left[4.1 \left(\frac{R}{1 \mu\text{m}} \right)^{-5} + 0.3 \right]^{-1}. \quad (7)$$

In contrast, we note that Earth’s deep biosphere has been estimated to comprise a total biomass of roughly 20 Pg C (Magnabosco et al. 2018, pg. 712), which would translate to a total biomass of $\sim 6 \times 10^{13} \text{ kg}$, after using a dry-to-total biomass conversion factor of 3 (Bratbak & Dundas 1984). Hence, this translates to $\sigma_{\oplus} \approx 1.2 \times 10^{-1} \text{ kg m}^{-2}$ for Earth’s deep biosphere after employing a cross-sectional area of $4\pi R_{\oplus}^2$. It is not surprising that (7) is a few orders of magnitude smaller than σ_{\oplus} , because the former is derived under the assumption of a relatively high ϵ as elucidated earlier. On the other hand, if one considers $P_{\text{bio}} \sim P_{\text{min}}$ (which effectively amounts to $\epsilon \ll 1$), corresponding to primarily sessile microbes such as those ostensibly existent in the deep biosphere, it is straightforward for σ_{max} to be comparable to σ_{\oplus} .

In Figure 1, we have plotted σ_{max} for the Martian subsurface and for the ocean of Enceladus as a function of R . The reason for choosing the latter environment is that molecular hydrogen was confirmed in the plumes of Enceladus by the *Cassini* mission (Waite et al. 2017). We adopt $|\Delta G| \approx 80 \text{ kJ mol}^{-1}$ and $\Phi_{\text{max}} \approx 1.2 \times 10^{12} \text{ m}^{-2} \text{ s}^{-1}$ on the basis of the combined empirical constraints and geochemical modeling presented in Waite et al. (2017). Note that Φ_{max} is higher than Φ_M by nearly two orders of magnitude because Enceladus is anticipated to have active hydrothermal processes.

As a consequence, it is evident from Figure 1 that $\sigma_{\text{max}} > \sigma_{\oplus}$ for $R > 1 \mu\text{m}$, although it is a few times smaller than Earth’s surface biomass density of $\sim 3.2 \text{ kg m}^{-2}$, the latter of which is derived after invoking the biomass estimates from Bar-On et al. (2018). It is apparent from the figure that σ_{max} increases with the size until it eventually saturates, in accordance with (7). The lower bound of R in all the figures is specified to be $\sim 0.1 \mu\text{m}$ due to biophysical constraints (Morowitz 1967; Martens et al. 2015), although it may be a few times higher when additional constraints on gradient sensing are taken into account (Dusenbery 2009; Lingam 2021).

At this stage, an important point is worth reiterating. We have only examined the energetic costs directly stemming from the act of locomotion. In other

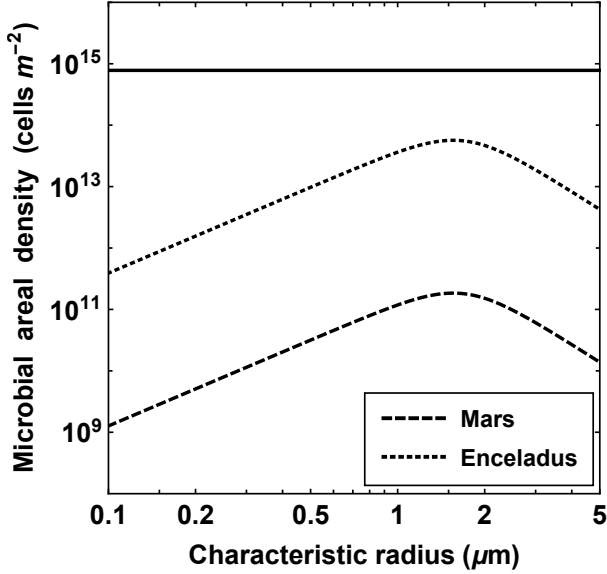


Figure 2. The upper bound on the column number density (i.e., microbes per unit area) of motile microbes in SI units of cells m^{-2} as a function of the microbe radius (in μm) for putative methanogens in the Martian subsurface and the ocean of Enceladus. These estimates were calculated for the fiducial choice of $\epsilon \sim 0.1$ in (8), which is the fraction of time spent in motion. The horizontal black line is an estimate of the column density of Earth’s deep biosphere.

words, we have not studied the auxiliary costs involved with motility like the manufacture of flagella and cilia. Empirical evidence suggests that the majority of the energetic costs for reasonably active microbes are attributable to locomotion (i.e., they are enshrined in P_m), implying that our analysis might represent a reasonable approximation for this class of organisms (see Taylor & Stocker 2012; Kempes et al. 2017).

Instead of plotting the biomass areal density, it is possible to calculate the column number density of cells η_{\max} (units of cells m^{-2}) instead. This quantity is determined by dividing σ_{\max} , which is given by (7), by C_{cell} . As a consequence, we end up with

$$\eta_{\max} \approx 5.2 \times 10^{11} \text{ cells } m^{-2} \left(\frac{\Phi_{\max}}{\Phi_M} \right) \left(\frac{|\Delta G|}{|\Delta G_M|} \right) \times \left(\frac{\epsilon}{0.1} \right)^{-1} \left[4.1 \left(\frac{R}{1 \mu m} \right)^{-2} + 0.3 \left(\frac{R}{1 \mu m} \right)^3 \right]^{-1} \quad (8)$$

For comparison, when it comes to Earth’s deep biosphere, it contains approximately 4×10^{29} cells (Magnabosco et al. 2018, pg. 707) over an area of $4\pi R_{\oplus}^2$. Hence, the column number density of microbes in Earth’s deep biosphere is $\eta_{\oplus} \approx 7.8 \times 10^{14}$ cells m^{-2} . For the fiducial values chosen above, it is apparent that $\eta_{\max} \ll \eta_{\oplus}$, but this condition does not hold true when ϵ drops several orders of magnitude below unity.

Figure 2 illustrates η_{\max} as a function of R for the Martian subsurface and the ocean of Enceladus, along the lines of Figure 1. There are a couple of interesting points that emerge from this figure. First, for the appropriate choice of ϵ , we notice that η_{\oplus} is comfortably higher than η_{\max} for all values of R . As explained previously, this trend is not surprising given that most microbes in Earth’s deep biosphere are sessile and characterized by $P_{\text{bio}} \sim P_{\text{min}}$. Second, η_{\max} is a nonmonotonic function of R and attains a maximum value at $R = R_c$, the latter of which was derived earlier. The reason stems from the fact that $\eta_{\max} \propto 1/P_m$ in our model.

Last, if the motile microbes are assumed to be uniformly mixed throughout the typical column depth H of the solvent, the number density of microbes \mathcal{N}_{\max} can be estimated as follows:

$$\mathcal{N}_{\max} \approx \frac{\eta_{\max}}{H}. \quad (9)$$

It is, however, not easy to gauge the magnitude of H for the Martian subsurface because what matters is not the total depth of the subsurface habitable region, but the fraction of that depth composed of the solvent in which the putative microbes dwell, which is hard to ascertain. If we consider the ocean of Enceladus, it may be a reasonable approximation to suppose that, over the span of geological timescales, microbes inhabit the entirety of its ocean, thereby amounting to $H \approx 40$ km (Beuthe et al. 2016; Hemingway & Mittal 2019).

Hence, in the case of Enceladus, by adopting the above value of H and making use of (8) and (9), it is possible to calculate \mathcal{N}_{\max} . For the basis of comparison, it is instructive to invoke the total microbial number densities associated with some of the harsher environments on Earth. Subglacial lakes (e.g., Lake Grímsvötn in Greenland and Lake Vostok in Antarctica) exhibit densities of $\gtrsim 10^8 - 10^{10}$ cells m^{-3} (Parnell & McMahon 2016, Table 1), the deep-ocean sediments of the North Pacific Gyre are characterized by $\sim 10^9$ cells m^{-3} (Orcutt et al. 2011; Røy et al. 2012), and groundwater extracted from granitic rocks ~ 3 km below the surface evinces densities of $\gtrsim 10^{10}$ cells m^{-3} (Lin et al. 2006, Table 1).

On the basis of the above paragraph, a cell density of $\rho_{\oplus} \approx 10^9$ cells m^{-3} is a good measure of the *total* (i.e., motile and sessile) microbial number density in extreme habitats on Earth. In Figure 3, we have plotted \mathcal{N}_{\max} as a function of R and contrasted it against ρ_{\oplus} . We caution that \mathcal{N}_{\max} is exclusively for motile organisms, whereas ρ_{\oplus} is composed of both motile and immobile microbes. There are a couple of aspects that stand out. First, on account of the fact that $\mathcal{N}_{\max} \propto 1/P_m$, it follows that the number density attains a maximum at $R = R_c$. Second, and more importantly, we discover that \mathcal{N}_{\max} is close to ρ_{\oplus} under near-optimal circumstances, but is otherwise roughly an order of magnitude (or more) smaller than the latter. Hence, this would suggest that

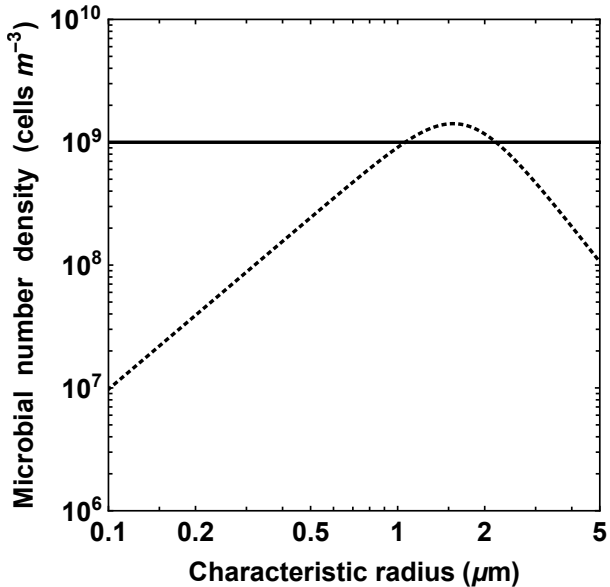


Figure 3. The upper bound on the number density (i.e., microbes per unit volume) of motile microbes in SI units of cells m^{-3} as a function of the microbe radius (in μm) for putative methanogens in the ocean of Enceladus. These estimates were derived for the fiducial choice of $\epsilon \sim 0.1$, which is the fraction of time spent in motion. The horizontal black line embodies the characteristic *total* (i.e., motile and sessile) microbial number densities documented for extreme environments on Earth.

the average density of motile microbes in the ocean of Enceladus might end up being very low.

In closing, we note that it is feasible to calculate the mass density of microbes by dividing σ_{\max} with H and plugging in the numbers of Enceladus. We have, however, opted not to do so because most studies tend to focus on determining or estimating \mathcal{N}_{\max} , both in Earth-based and extraterrestrial habitats.

4. CONCLUSION

It is well-known that motility represents a genuine biosignature candidate (Nadeau et al. 2016), and that it accords microbes a number of adaptive benefits. Hence, motivated by these considerations, we explored the prospects for motility in astrobiological environments.

We began by showing that run-and-tumble chemotaxis, the *de facto* mode of motility under many circumstances, is rendered optimal in terms of power consumption when the microbes have radii of $\sim 1.6 \mu m$. Next, by making use of a simple bioenergetic model wherein the vast majority of the available free energy is directed toward enabling motility, we assessed the maximum amount of biomass that could exist in the form of motile organisms. In particular, we calculated the global integrated biomass density per unit area σ_{\max} , the column number density η_{\max} (number of microbes

per unit area) and the number density \mathcal{N}_{\max} (number of microbes per unit volume) of microbes, with the last result following from the additional postulate of uniform mixing.

We applied our results to the Martian subsurface and to the ocean of Enceladus. We focused on methanogens as these organisms have been well studied on Earth and they require access to molecular hydrogen, which is believed to be prevalent in both locales. Among other results, we showed that the estimates for η_{\max} for both Mars and Enceladus are likely to be lower than the corresponding value for Earth’s deep biosphere. We also demonstrated that \mathcal{N}_{\max} in the ocean of Enceladus is potentially smaller than the total number density of microbes across myriad harsh environments on Earth.

As with any model, there are some potential caveats in need of highlighting. First, our analysis was conducted for a particular variant of motility (run-and-tumble chemotaxis). Adopting a different mode would give rise to changes in the scalings, although the magnitudes of the relevant variables might remain similar (Mitchell 2002). Second, our model set aside the metabolic requirements for basal maintenance and the synthesis of swimming appendages (e.g., flagella and cilia), which is why all of our predictions constitute upper bounds; the actual values may consequently end up being much smaller.

Third, as our model was predicated on tackling only energetic constraints, it ignored the possibility that nutrient limitations could act to suppress the biomass further. More specifically, theoretical modeling by Lingam & Loeb (2018, 2019) indicates that phosphorus limitation might engender additional bottlenecks insofar as Enceladus is concerned. Fourth, our estimates represent global averages, and therefore do not account for spatial heterogeneity, for example, hotspots wherein free energy sources and/or nutrients are concentrated and lead to the clustering of microbes. In order to model the actual density of motile organisms at such locations, it would be necessary to modify Φ_{\max} and $|\Delta G|$ accordingly. However, this remains a challenging enterprise in the current epoch, given our limited empirical data regarding the (sub)surface environments of habitable worlds in the Solar system.

In spite of these ostensible drawbacks, our model nevertheless has two major advantages, which were adumbrated in Sec. 1. The first is that it enables us to at least achieve a rough understanding of the global cell densities of mobile microorganisms to anticipate in future astrobiological missions and to plan for such eventualities. Second, our results are transparent due to the relative simplicity of the model and can therefore be readily assessed and falsified by forthcoming life-detection experiments. It is thus our hope and expectation that this work will pave the way for quantifying the prospects for motility in extraterrestrial milieu.

ACKNOWLEDGMENTS

We are grateful to Chris McKay and an anonymous reviewer for their meticulous and insightful reviews of the paper, which were helpful for improving the manuscript. This research was supported in part by the Breakthrough Prize Foundation, Harvard University’s Faculty of Arts and Sciences, and the Institute for Theory and Computation (ITC) at Harvard University.

APPENDIX

A. CHALLENGES AND RATIONALE FOR MODELING RUN-AND-TUMBLE CHEMOTAXIS

Many studies that have attempted to gauge the energetic costs associated with basic physiological functions of microbes tend to use run-and-tumble locomotion on account of its applicability to environments with low Reynolds numbers (Berg 1993; Kempes et al. 2017, 2019). Although run-and-tumble chemotaxis is often perceived as being apropos for nutrient-rich habitats, there are two caveats that should be recognized.

1. Observational data concerning the availability and abundance of bioessential nutrients in most astrobiological environments is very scarce. For example, while the Cassini mission collected evidence favoring the existence of nitrogenous compounds during its passage through the plume of Enceladus (Postberg et al. 2018), the abundance of phosphorus-based species remains unknown due to the absence of empirical data. Hence, it is not inconceivable that some of these settings have more nutrients than expected and are primarily energy-limited.
2. Run-and-tumble chemotaxis is anticipated to be functional even in low-nutrient environments, such as those inhabited by halophilic archaea on Earth (Thornton et al. 2020).

Looking beyond the issue of nutrient abundance, there are multiple chemotactic strategies that are accessible. There are, however, other uncertainties that arise in this context, which are explicated below.

1. There are substantive differences in how motility is effectuated in bacteria and archaea, but our understanding of swimming and other related properties of the latter is still much less understood than the former (Herzog & Wirth 2012).
2. If we specialize to bacteria, there are a diverse array of chemotactic strategies that are feasible such as run-and-tumble, run-and-arc, run-and-reverse, run-tumble-flick, and run-reverse-flick.
3. If we further consider only a single parameter, even in this restricted case, we are confronted with much heterogeneity. For instance, increased phosphorylation of the CheY protein inhibits tumbling in gram-positive *Bacillus subtilis*, whereas the converse is valid for gram-negative *Escherichia coli* (Garrity & Ordal 1995).
4. In connection with the above point, the swimming speed of a given organism can vary by a factor of order unity owing to its propensity to modulate its locomotion when travelling forward or backward, as seen from the example of the soil bacterium *Pseudomonas putida* (Theves et al. 2013).

In light of the preceding considerations, it may be argued that a first attempt at estimating the biomass density of motile microbes should attempt to construct a model endowed with sufficient simplicity and generality. A heuristic model can subsequently pave the way for more complex analyses of this pertinent subject, as contended in Sec. 4. It is apparent that the basic version of run-and-tumble chemotaxis—which applies to a spherical swimmer—has the requisite property of simplicity (Kempes et al. 2019). Now, when it comes to addressing the question of generality, it is necessary to compare run-and-tumble locomotion with other strategies; we will mostly draw upon the results derived in Mitchell (2002), except when stated otherwise.

1. For organisms with radii of $\gtrsim 1 \mu\text{m}$, the length and aspect ratio of the flagellum do not significantly influence the power requirements for run-and-tumble locomotion; in other words, the power expended varies merely by a factor of order unity.
2. For organisms characterized by $R \gtrsim 0.8 \mu\text{m}$, the power requirements for run-and-tumble locomotion are rendered almost independent of the length scales associated with the chemical gradients pertaining to chemotaxis.

3. The power requirements for run-and-tumble and run-and-arc locomotion are within an order of magnitude of each other, provided that the radius of the microbe is $\lesssim 10 \mu\text{m}$.
4. In the range of $R \gtrsim 0.5 \mu\text{m}$, it is plausible that the run-and-tumble and run-and-reverse modes of locomotion have comparable power requirements.
5. The mean squared displacement for run-and-tumble, run-and-reverse, and run-reverse-flick is within an order of magnitude even over a timescale that is ~ 100 times the mean run time (Taktikos et al. 2013).
6. For many bacteria (e.g., *Escherichia coli*), the predicted chemotactic drift speeds are similar for run-and-tumble, run-tumble-flick, and run-reverse-flick modes of locomotion (Taktikos et al. 2013).

As indicated by these points, run-and-tumble locomotion might possess a certain degree of generality, implying that the results derived in the paper may also be imbued with some validity. Furthermore, the range of radii described above overlap, for the most part, with the radii at which the biomass variables in Figures 1–3 reach their maximal values. We reiterate, however, that our analysis is not meant to be definitive and could thus serve as a stepping stone for more sophisticated treatments of this subject in the future.

REFERENCES

- Azam, F., & Malfatti, F. 2007, *Nat. Rev. Microbiol.*, 5, 782, doi: [10.1038/nrmicro1747](https://doi.org/10.1038/nrmicro1747)
- Bar-On, Y. M., Phillips, R., & Milo, R. 2018, *Proc. Natl. Acad. Sci. USA*, 115, 6506, doi: [10.1073/pnas.1711842115](https://doi.org/10.1073/pnas.1711842115)
- Berg, H. C. 1993, *Random Walks in Biology*, 2nd edn. (Princeton: Princeton University Press)
- Beuthe, M., Rivoldini, A., & Trinh, A. 2016, *Geophys. Res. Lett.*, 43, 10,088, doi: [10.1002/2016GL070650](https://doi.org/10.1002/2016GL070650)
- Bradley, J. A., Arndt, S., Amend, J. P., et al. 2020, *Sci. Adv.*, 6, eaba0697, doi: [10.1126/sciadv.aba0697](https://doi.org/10.1126/sciadv.aba0697)
- Bratbak, G., & Dundas, I. 1984, *Appl. Environ. Microbiol.*, 48, 755
- Dusenbery, D. B. 2009, *Living at Micro Scale: The Unexpected Physics of Being Small* (Cambridge: Harvard University Press)
- Fenchel, T. 2008, *Aquat. Microb. Ecol.*, 51, 23, doi: [10.3354/ame01182](https://doi.org/10.3354/ame01182)
- Garrity, L. F., & Ordal, G. W. 1995, *Pharmacol. Ther.*, 68, 87, doi: [10.1016/0163-7258\(95\)00027-5](https://doi.org/10.1016/0163-7258(95)00027-5)
- Hand, K. P., Sotin, C., Hayes, A., & Coustenis, A. 2020, *Space Science Reviews*, 216, 1, doi: [10.1007/s11214-020-00713-7](https://doi.org/10.1007/s11214-020-00713-7)
- Hemingway, D. J., & Mittal, T. 2019, *Icarus*, 332, 111, doi: [10.1016/j.icarus.2019.03.011](https://doi.org/10.1016/j.icarus.2019.03.011)
- Herzog, B., & Wirth, R. 2012, *Appl. Environ. Microbiol.*, 78, 1670, doi: [10.1128/AEM.06723-11](https://doi.org/10.1128/AEM.06723-11)
- Higgins, P. M., & Cockell, C. S. 2020, *J. R. Soc. Interface*, 17, 20200588, doi: [10.1098/rsif.2020.0588](https://doi.org/10.1098/rsif.2020.0588)
- Hoehler, T. M. 2007, *Astrobiology*, 7, 824, doi: [10.1089/ast.2006.0095](https://doi.org/10.1089/ast.2006.0095)
- Holz, M., Heil, S. R., & Sacco, A. 2000, *Phys. Chem. Chem. Phys.*, 2, 4740, doi: [10.1039/B005319H](https://doi.org/10.1039/B005319H)
- Kempes, C. P., Koehl, M. A. R., & West, G. B. 2019, *Front. Ecol. Evol.*, 7, 242, doi: [10.3389/fevo.2019.00242](https://doi.org/10.3389/fevo.2019.00242)
- Kempes, C. P., van Bodegom, P. M., Wolpert, D., et al. 2017, *Front. Microbiol.*, 8, 31, doi: [10.3389/fmicb.2017.00031](https://doi.org/10.3389/fmicb.2017.00031)
- Lever, M. A., Rogers, K. L., Lloyd, K. G., et al. 2015, *FEMS Microbiol. Rev.*, 39, 688, doi: [10.1093/femsre/fuv020](https://doi.org/10.1093/femsre/fuv020)
- Lin, L.-H., Wang, P.-L., Rumble, D., et al. 2006, *Science*, 314, 479, doi: [10.1126/science.1127376](https://doi.org/10.1126/science.1127376)
- Lingam, M. 2021, *Astrobiology*, arXiv:2102.05009. <https://arxiv.org/abs/2102.05009>
- Lingam, M., & Loeb, A. 2018, *Astron. J.*, 156, 151, doi: [10.3847/1538-3881/aada02](https://doi.org/10.3847/1538-3881/aada02)
- . 2019, *Int. J. Astrobiol.*, 18, 112, doi: [10.1017/S1473550418000083](https://doi.org/10.1017/S1473550418000083)
- . 2020, *Int. J. Astrobiol.*, arXiv:2009.07835. <https://arxiv.org/abs/2009.07835>
- . 2021, *Life in the Cosmos: From Biosignatures to Technosignatures* (Cambridge: Harvard University Press). <https://www.hup.harvard.edu/catalog.php?isbn=9780674987579>
- Magnabosco, C., Lin, L. H., Dong, H., et al. 2018, *Nat. Geosci.*, 11, 707, doi: [10.1038/s41561-018-0221-6](https://doi.org/10.1038/s41561-018-0221-6)
- Martens, E. A., Wadhwa, N., Jacobsen, N. S., et al. 2015, *Proc. R. Soc. B*, 282, 20151346, doi: [10.1098/rspb.2015.1346](https://doi.org/10.1098/rspb.2015.1346)
- McKay, C. P., & Smith, H. D. 2005, *Icarus*, 178, 274, doi: [10.1016/j.icarus.2005.05.018](https://doi.org/10.1016/j.icarus.2005.05.018)
- Michalski, J. R., Onstott, T. C., Mojzsis, S. J., et al. 2018, *Nat. Geosci.*, 11, 21, doi: [10.1038/s41561-017-0015-2](https://doi.org/10.1038/s41561-017-0015-2)
- Milo, R., & Phillips, R. 2016, *Cell Biology by the Numbers* (New York: Garland Science)

- Mitchell, J. G. 1991, *Microb. Ecol.*, 22, 227, doi: [10.1007/BF02540225](https://doi.org/10.1007/BF02540225)
- . 2002, *Am. Nat.*, 160, 727, doi: [10.1086/343874](https://doi.org/10.1086/343874)
- Mitchell, J. G., & Kogure, K. 2006, *FEMS Microbiol. Ecol.*, 55, 3, doi: [10.1111/j.1574-6941.2005.00003.x](https://doi.org/10.1111/j.1574-6941.2005.00003.x)
- Morowitz, H. J. 1967, *Prog. Theoret. Biol.*, 1, 35
- Nadeau, J., Lindensmith, C., Deming, J. W., Fernandez, V. I., & Stocker, R. 2016, *Astrobiology*, 16, 755, doi: [10.1089/ast.2015.1376](https://doi.org/10.1089/ast.2015.1376)
- Neveu, M., Anbar, A., Davila, A. F., et al. 2020, *Front. Astron. Space Sci.*, 7, 26, doi: [10.3389/fspas.2020.00026](https://doi.org/10.3389/fspas.2020.00026)
- Orcutt, B. N., Sylvan, J. B., Knab, N. J., & Edwards, K. J. 2011, *Microbiol. Mol. Biol. Rev.*, 75, 361, doi: [10.1128/MMBR.00039-10](https://doi.org/10.1128/MMBR.00039-10)
- Parnell, J., & McMahon, S. 2016, *Phil. Trans. R. Soc. A*, 374, 20140293, doi: [10.1098/rsta.2014.0293](https://doi.org/10.1098/rsta.2014.0293)
- Postberg, F., Khawaja, N., Abel, B., et al. 2018, *Nature*, 558, 564, doi: [10.1038/s41586-018-0246-4](https://doi.org/10.1038/s41586-018-0246-4)
- Riekeles, M., Schirmack, J., & Schulze-Makuch, D. 2021, *Life*, 11, 44, doi: [10.3390/life11010044](https://doi.org/10.3390/life11010044)
- Røy, H., Kallmeyer, J., Adhikari, R. R., et al. 2012, *Science*, 336, 922, doi: [10.1126/science.1219424](https://doi.org/10.1126/science.1219424)
- Seager, S., Bains, W., & Hu, R. 2013, *Astrophys. J.*, 775, 104, doi: [10.1088/0004-637X/775/2/104](https://doi.org/10.1088/0004-637X/775/2/104)
- Shock, E. L., & Holland, M. E. 2007, *Astrobiology*, 7, 839, doi: [10.1089/ast.2007.0137](https://doi.org/10.1089/ast.2007.0137)
- Sholes, S. F., Krissansen-Totton, J., & Catling, D. C. 2019, *Astrobiology*, 19, 655, doi: [10.1089/ast.2018.1835](https://doi.org/10.1089/ast.2018.1835)
- Stocker, R. 2012, *Science*, 338, 628, doi: [10.1126/science.1208929](https://doi.org/10.1126/science.1208929)
- Taktikos, J., Stark, H., & Zaburdaev, V. 2013, *PLoS ONE*, 8, e81936, doi: [10.1371/journal.pone.0081936](https://doi.org/10.1371/journal.pone.0081936)
- Taubner, R.-S., Schleper, C., Firneis, M. G., & Rittman, S. K. M. R. 2015, *Life*, 5, 1652, doi: [10.3390/life5041652](https://doi.org/10.3390/life5041652)
- Taubner, R.-S., Pappenreiter, P., Zwicker, J., et al. 2018, *Nat. Commun.*, 9, 748, doi: [10.1038/s41467-018-02876-y](https://doi.org/10.1038/s41467-018-02876-y)
- Taylor, J. R., & Stocker, R. 2012, *Science*, 338, 675, doi: [10.1126/science.1219417](https://doi.org/10.1126/science.1219417)
- Theves, M., Taktikos, J., Zaburdaev, V., Stark, H., & Beta, C. 2013, *Biophys. J.*, 105, 1915, doi: [10.1016/j.bpj.2013.08.047](https://doi.org/10.1016/j.bpj.2013.08.047)
- Thornton, K. L., Butler, J. K., Davis, S. J., Baxter, B. K., & Wilson, L. G. 2020, *Nat. Commun.*, 11, 4453, doi: [10.1038/s41467-020-18253-7](https://doi.org/10.1038/s41467-020-18253-7)
- Van Bodegom, P. 2007, *Microb. Ecol.*, 53, 513, doi: [10.1007/s00248-006-9049-5](https://doi.org/10.1007/s00248-006-9049-5)
- Waite, J. H., Glein, C. R., Perryman, R. S., et al. 2017, *Science*, 356, 155, doi: [10.1126/science.aai8703](https://doi.org/10.1126/science.aai8703)
- Wray, J. J. 2021, *Annu. Rev. Earth Planet. Sci.*, 49, doi: [10.1146/annurev-earth-072420-071823](https://doi.org/10.1146/annurev-earth-072420-071823)